

Optical Faraday effect due to spin-density fluctuations of electrons in *n*-type semiconductors

E. Yu. Perlin and A. M. Danishevskii

All-Russia Scientific Center "S.I. Vavilov State Optical Institute", 199034 St. Petersburg, Russia
(Submitted 23 November 1993; resubmitted 25 April 1994)
Zh. Eksp. Teor. Fiz. **106**, 503–521 (August 1994)

The optical Faraday effect (induced rotation of the polarization plane of probe light induced by circularly polarized pump radiation) is studied theoretically and experimentally. The effect is described using the third-order susceptibility, which is calculated by means of the Hamiltonian for the effective interaction between the electron system of the semiconductor and the light, including virtual interband transitions with spin flip. The equations of motion for the Green's function are solved in the random phase approximation. It is shown that in *n*-type A_3B_5 materials in the infrared region of the spectrum far from one- or two-photon interband resonances, the main contribution to induced rotation of the polarization comes from a mechanism associated with fluctuations of the electron spin density in the conduction band. Measurements have been made in *n*-InAs and *n*-InSb samples with different amounts of doping. The magnitude of the effect and its density dependence vary, depending on whether the probe radiation and the pump propagate in the same or opposite directions. A resonant increase in the rotation angle of the polarization is observed as the spin splitting of the conduction band at the Fermi level approaches the frequency difference of the two light waves. All the observed properties of the effect agree qualitatively with the results of theory.

1. INTRODUCTION

When linearly polarized probe radiation with frequency Ω propagates in a medium in the presence of intense circularly polarized pump radiation with frequency ω , the plane of polarization of the probe radiation is rotated by an angle θ proportional to the intensity of the pump.^{1–3} This phenomenon, which is due to the cubic susceptibility of the medium, is usually called the optical Faraday effect (OFE). In the presence of isotropic linear absorption (absorption coefficient α) for right-polarized pump radiation propagating in the *z* direction, the rotation angle θ is given by the following expression in terms of the Cartesian components of the third-order susceptibility $\chi^{(3)}$:

$$\theta = \alpha^{-1}(\omega) \{1 - \exp[-\alpha(\omega)d]\} I_\omega \bar{\theta} \cos \psi, \quad (1)$$

$$\bar{\theta} = \frac{4\pi^2\Omega}{c^2\kappa_0^2(\Omega)} \chi^{(a)},$$

$$\chi^{(a)} = \text{Re}[\chi_{1212}^{(3)}(\Omega; \Omega, \omega, -\omega) - \chi_{1221}^{(3)}(\Omega; \Omega, \omega, -\omega)], \quad (2)$$

where ψ is the angle between the directions of propagation of the pump and probe, which we assume to be close to either 0 or π ; $\kappa_0(\Omega)$ is the index of refraction; I_ω is the intensity of the pump in the medium at its leading edge; and d is the distance over which the pump and probe radiation propagate through the medium. For purely monochromatic pump and probe radiation the magnitude of the OFE does not depend on the phase relations between the fields, since the intensity \mathbf{F}_ω of the field of a wave ω enters into all expressions in the form of a combination which is bilinear in \mathbf{F}_ω^* and \mathbf{F}_ω , so that the phase factors drop out. Thus, the gyration pseudovector⁴ satisfies

$$\mathbf{g} \propto i(\mathbf{F}_\omega \times \mathbf{F}_\omega^*).$$

If, on the other hand, the pump and probe signals in an experiment consist of superpositions of several radiation lines, then the situation becomes more complicated. We return to this point below.

The OFE was studied theoretically by Perlin⁵ in intrinsic crystals with a Kane square-root dispersion law for the bands. There it was shown that the magnitude of the induced rotation of the polarization satisfies $\theta \propto E_g^{-7/2}$ (here E_g is the width of the bandgap in the crystal). At the same time the expression for θ includes terms proportional to $(E_g - \hbar\Omega - \hbar\omega)^{-3/2}$, so that the polarization rotation angles are largest near the threshold for two-photon absorption of the fundamental. In the list of materials suitable for observation of the OFE it is natural to include A_3B_5 materials with small values of E_g , which are well described by the Kane band-structure model. Indeed, the first observations of the OFE in semiconductors were made in InAs crystals,⁶ where the measurements were carried out using CO_2 laser radiation and its second harmonic. It became apparent that the magnitude of the OFE increases as $\hbar\omega + \hbar\Omega$ approached E_g rather more slowly than the theory of Ref. 5 predicts. Moreover, it was shown in Ref. 6 that the rotation angle θ increases as the probe radiation frequency approaches that of the pump. This implies that a nonlinear mechanism is involved, associated with the free carriers present in the material: in all samples investigated the density n_0 of the free electrons was greater than 10^{16} cm^{-3} .

There are various OFE mechanisms associated in one way or another with the presence of free electrons. One of these arises from the population of states with momentum p less than the Fermi momentum p_F that are located at the bottom of the conduction band. This can result in a consid-

erable change in the interband nonlinear susceptibility (in analogy with the Moss–Burstein effect in light absorption). What happens is that the main contribution to $\chi^{(3)}$ in this case comes from a narrow range of states with $p \ll (2m_c E_g)^{1/2}$, and this contribution is suppressed as the bottom of the band fills up. The interband OFE mechanism dominates in two-photon interband resonance, which makes the dependence of the induced rotation angle of the polarization on the electron density n_0 quite nontrivial (cf. Ref. 7). When the sum of the probe and pump frequencies is small in comparison with E_g , there is a nonlinear mechanism associated with the nonparabolic shape of the electron band spectrum.^{8,9} This mechanism, however, does not contribute to the susceptibility combination (2), just like the nonlinear mechanisms associated with heating of the carriers by the pump radiation and their relaxation.^{10,11}

As early as 1963 Butcher and McLean⁸ pointed out another type of optical nonlinearity in semiconductors, associated with fluctuations in the electron gas density. Sections 2 and 3 are devoted to the fluctuation mechanism of nonlinearity. We will show that the main contribution to $\chi^{(a)}$ comes from fluctuations in the electron spin density, which in contrast to “ordinary” electron density fluctuations carry no charge and therefore are not suppressed by shielding at high densities n_0 of the free electrons. The spin-density fluctuation mechanism differs qualitatively from the OFE mechanisms mentioned previously in the following ways: a) it has a very different dependence on the density; b) the magnitude of the effect associated with the spin-density fluctuation mechanism depends qualitatively on the probe and pump wave vectors, in particular in the appearance of differences in the respective magnitude and density dependence for propagation of the pump and probe in parallel and antiparallel directions; c) the polarization rotation angle depends strongly on the structure of the laser radiation spectrum; d) the magnitude of the OFE may be determined by the magnitude of the spin splitting of the conduction band proportional to the cube of the momentum.

We reported the first results on the OFE induced by spin-density fluctuations in Ref. 12.

In the case of molecular systems or for the interband nonlinear mechanism in semiconductors, the OFE is close to its classical analog. The difference is that the constant magnetic field \mathbf{H} in the ordinary Faraday effect is replaced in the OFE by a quantity proportional to $\mathbf{F}_\omega \times \mathbf{F}_\omega^*$. As in the ordinary Faraday effect, in the OFE when the probe radiation propagates forward and backward (with the direction of the pump remaining unchanged), the rotation angle of the plane of polarization of the probe radiation doubles. In the fluctuation nonlinear mechanism, however, the situation is more complicated because of the occurrence of spatial dispersion noted above. Nevertheless, in this case also the effect we are considering still resembles the Faraday effect more closely than the natural optical activity directly associated with the presence of spatial dispersion.

Thus far we have discussed OFE mechanisms for which no actual change occurs in the occupation numbers in the electronic system of the semiconductor. However, the plane of polarization of the probe radiation can also undergo

photoinduced rotation as a result of spin orientation of electrons or holes. This occurs for one- or two-photon interband transitions, indirect transitions involving phonons within the conduction band through virtual states in the valence band, or for transitions between subbands of a complex valence band due to the action of a circularly polarized pump. The latter mechanism was studied theoretically and experimentally by Danishevskii *et al.*¹³ At very low temperatures, spin splitting of the conduction band can also occur through interaction with the pump [see the effective Hamiltonian (17) in Sec. 2]. However, under the conditions of the experiments described in the present work the role of such mechanisms is minor (see Sec. 5).

In principle, all OFE mechanisms can be encompassed by a unified approach. But in practice this treatment is found to be unacceptably involved, since in the above cases the method of calculation most suited to the physics underlying a particular mechanism is different in each instance. In the present work we therefore restrict ourselves mainly to treating the situation where the spin-density fluctuation mechanism dominates. The effective Hamiltonian $\hat{H}^{(2)}$ for the interaction of the crystal electron system with light will be used (see, e.g., Ref. 14, Ch. 5). This Hamiltonian permits the problem to be treated in a natural way in terms of the charge and spin-density fluctuations of the free electrons. It is not obvious *a priori*, however, that $\hat{H}^{(2)}$ includes all processes which in principle might contribute significantly to the OFE. In the derivation of $\hat{H}^{(2)}$ in Sec. 2 all possible fourth-order terms in the light fields are included in the expression for the internal energy of the electron system of the crystal, and it is shown that the terms not described by the effective Hamiltonian are negligible for this nonlinear mechanism. Then in Sec. 3 we use the interband Coulomb interaction and the interaction between the electrons and the longitudinal optical phonons in the random-phase approximation to derive and solve the equations of motion for the Green’s functions in terms of which the angle of induced rotation of the probe-wave polarization is ultimately expressed. This type of approach, similar to that employed previously in a number of treatments of Raman scattering in A_3B_5 semiconductor plasmas (see, e.g., Refs. 14 and 15) enables us to treat the role of shielding in the electron system in a systematic way. Furthermore, this approach enables us to treat such delicate effects as the spin splitting of the conduction band to third order in the electron momentum. Inclusion of this splitting has a fundamental importance, since in a number of cases it determines the amplitude and the density dependence of the OFE. The experimental technique is described in Sec. 4. The results of experiments for InAs and InSb crystals, along with a qualitative interpretation based on the theory developed in Secs. 2 and 3 are presented in Sec. 5.

2. EFFECTIVE INTERACTION HAMILTONIAN

The Hamiltonian \hat{H} of the electron system in the field of electromagnetic radiation takes the form

$$\hat{H} = \hat{H}_{el} + \hat{H}' + \hat{H}'', \quad (3)$$

$$\hat{H}_{el} = \sum_{\mathbf{k}, i} \mathcal{E}_i(\mathbf{k}) \zeta_{i\mathbf{k}}^+ \zeta_{i\mathbf{k}}, \quad (4)$$

$$\begin{aligned} \hat{H}' = \sum_{\mathbf{k}, i, j, \lambda} & (\mathcal{V}_{\mathbf{k}i; \mathbf{k}+\mathbf{\kappa}j}^{\mu} \mathcal{A}_{\mu}(\omega_{\lambda}) e^{-i\omega_{\lambda}t} \zeta_{i\mathbf{k}}^+ \zeta_{j\mathbf{k}+\mathbf{\kappa}} \\ & + \mathcal{V}_{\mathbf{k}i; \mathbf{k}-\mathbf{\kappa}j}^{\mu} \mathcal{A}_{\mu}^*(\omega_{\lambda}) e^{i\omega_{\lambda}t} \zeta_{i\mathbf{k}}^+ \zeta_{j\mathbf{k}-\mathbf{\kappa}}). \end{aligned} \quad (5)$$

Here $\mathcal{E}_i(\mathbf{k})$ is the Bloch energy of the i th band (in the absence of the field). The creation and annihilation operators $\psi_{i\mathbf{k}}^+$, $\psi_{i\mathbf{k}}$ for states with wave vector \mathbf{k} in the i th band are replaced by the electron operators $a_{\mathbf{k}}^+$, $a_{i\mathbf{k}}$ or the hole operators $b_{i\mathbf{k}}$, $b_{i\mathbf{k}}^+$ where the subscript i runs through values corresponding to the conduction or valence bands; $\mathcal{A}_{\mu}(\omega_{\lambda})$ are the Cartesian coordinates of the amplitudes of the vector potentials; $\mathcal{V}_{\mathbf{k}i; \mathbf{k}'j}^{\mu}$ are the matrix elements of the Cartesian components of the operator

$$\pi = \mathbf{p} + \frac{\hbar}{4mc^2} (\boldsymbol{\sigma} \times \nabla V), \quad (6)$$

where $\boldsymbol{\sigma}$ is the Pauli matrix and V is the periodic lattice potential. For conciseness in (5) and also in (9) we have omitted the subscript λ from the wave vectors $\mathbf{\kappa}_{\lambda}$ corresponding to the light fields with frequencies ω_{λ} . Quantization in Eqs. (4) and (5) is based on the unperturbed Bloch functions. As can easily be shown (see, e.g., Ref. 14, Ch. 5) inclusion of the term \hat{H}'' in Eq. (3), which is quadratic in the field, gives rise to a small correction $\sim m_c/m$ (here m_c is the electron effective mass in the conduction band; in InAs $m_c \approx 0.02 m$) in the effective interaction Hamiltonian. In order not to complicate the presentation excessively we will therefore temporarily disregard H'' , and will later insert it into the effective Hamiltonian.

In the calculations below it is convenient to transform the original Hamiltonian (3)–(5):

$$\bar{H} = \exp(-\hat{S}) \hat{H} \exp(\hat{S}) - i \frac{\partial \hat{S}}{\partial t}. \quad (7)$$

The operator \hat{S} is chosen so that \bar{H} has no terms that are off-diagonal (od) in the band indices and linear in the field:

$$[\hat{H}_{el}, \hat{S}]_{od} + \hat{H}'_{od} - i \frac{\partial \hat{S}}{\partial t} = 0. \quad (8)$$

The condition (8) is satisfied by the operator

$$\begin{aligned} \hat{S} = \sum_{\substack{i, j \\ \mathbf{k}, \lambda}} & \left\{ \frac{\zeta_{i\mathbf{k}}^+ \zeta_{j\mathbf{k}+\mathbf{\kappa}} \mathcal{V}_{\mathbf{k}i; \mathbf{k}+\mathbf{\kappa}j}^{\mu} \mathcal{A}_{\mu}(\omega_{\lambda}) e^{-i\omega_{\lambda}t}}{\mathcal{E}_j(\mathbf{k}+\mathbf{\kappa}) - \mathcal{E}_i(\mathbf{k}) + \hbar\omega_{\lambda}} \right. \\ & \left. + \frac{\zeta_{i\mathbf{k}}^+ \zeta_{j\mathbf{k}-\mathbf{\kappa}} \mathcal{V}_{\mathbf{k}i; \mathbf{k}-\mathbf{\kappa}j}^{\mu} \mathcal{A}_{\mu}(\omega_{\lambda}) e^{i\omega_{\lambda}t}}{\mathcal{E}_j(\mathbf{k}-\mathbf{\kappa}) - \mathcal{E}_i(\mathbf{k}) - \hbar\omega_{\lambda}} \right\}. \end{aligned} \quad (9)$$

Transformations such as (7)–(9) have frequently been employed in semiconductor theory, starting with the work of Luttinger and Kohn.¹⁶ A modified technique for using the transformation (7)–(9) to calculate high-order nonlinear optical processes was developed by Ganichev *et al.*¹⁷

We introduce the density operator

$$\hat{\rho} = \exp(-i\hat{H}t/\hbar) \rho_0 \exp(i\hat{H}t/\hbar) \quad (10)$$

and write down the expression for the internal energy of the electron system in the field of the light waves:

$$\begin{aligned} u &= \text{Sp}\{\hat{\rho} \hat{H}_{el}\} = \text{Sp}\{\rho_0 \hat{H}_{el}\} - Q, \\ Q &\equiv \text{Sp} \left\{ \sum_{i=1}^{\infty} \rho^{(i)} H' \right\}, \end{aligned} \quad (11)$$

where $\rho^{(i)}$ is the i th term in the expansion of the density matrix in powers of the field. To get the components of the cubic susceptibility tensor $\chi^{(3)}$ it is necessary to calculate terms of fourth order in \mathcal{A}_{μ} entering into Q . We used the Hamiltonian (7), including terms of all orders in the field (see Ref. 17), as well as the technique for calculating the nonlinear reaction of the system to external perturbations.¹⁸ Without writing down the fourth-order terms explicitly we note that they can be constructed solely from the following combinations of the operators \hat{H}'_d , \hat{H}'_{od} , \hat{S} :

$$\begin{aligned} \text{I)} & \frac{1}{2} [\hat{H}'_{od}, \hat{S}] \cdot \frac{1}{2} [\hat{H}'_{od}, \hat{S}]; \quad \text{II)} \hat{H}'_d \cdot \frac{1}{2} [\hat{H}'_d, \hat{S}], \hat{S}; \\ \text{III)} & [\hat{H}'_d, \hat{S}] \cdot [\hat{H}'_d, \hat{S}]; \quad \text{IV)} \hat{H}'_d \cdot \hat{H}'_d \cdot \frac{1}{2} [\hat{H}'_d, \hat{S}]; \\ \text{V)} & \hat{H}'_d \cdot \hat{H}'_d \cdot \hat{H}'_d \cdot \hat{H}'_d. \end{aligned} \quad (12)$$

Now we must distinguish from among the contributions (12) those which are important specifically for the nonlinear mechanism of interest in the present work, associated with fluctuations in the density of free carriers. For this mechanism the quantity $\chi^{(3)}$ is determined by the state population at the bottom of the conduction band, corresponding to small values of the kinetic energy \mathcal{E}_{kin} . Under these conditions we can use the fact that the ratio $\beta \sim \sqrt{\mathcal{E}_{kin}/E_g}$ of the diagonal matrix elements of the operator \hat{H}' to the off-diagonal elements, corresponding to permitted interband transitions, is small (see, e.g., Ref. 19, Ch. 4 and App. 12), and neglect terms containing the operator \hat{H}'_d . Under other conditions these contributions can be quite significant. Thus, contribution III plays the dominant role in OFE for two-photon resonances of the form $\hbar\omega + \hbar\Omega \approx E_g$ in allowed-forbidden band transitions. This case was studied in detail in Refs. 5 and 7.

Generally speaking, fourth-order contributions in u can still arise because the density operator ρ_0 of the electron system without interactions also satisfies a transformation of the form (7):

$$\tilde{\rho}_0 = \rho_0 + [\rho_0, \hat{S}] + \frac{1}{2!} [[\rho_0, \hat{S}], \hat{S}] + \dots \quad (13)$$

We must, however, keep in mind that the fluctuation mechanism we are interested in applies only for identical or close wave frequencies interacting nonlinearly, when $\zeta_0 = |\omega_{\lambda} - \omega_{\lambda}| / (E_g/\hbar - \omega_{\lambda}) \ll 1$ holds. Calculating the contributions containing the commutators $[\rho_0, \hat{S}]$ which arise due to (13), we can easily convince ourselves that they are of order $\sim \zeta_0$ in comparison with I.

By virtue of these considerations it thus remains only to take into account contribution I. This implies in turn that the problem of calculating $\chi^{(a)}$ reduces to calculating u in first-

order perturbation theory with the Hamiltonian for the effective interaction between the electron system of the crystal and the electromagnetic fields:

$$\hat{H}^{(2)} = \frac{1}{2}[\hat{H}'_{\text{od}}, \hat{S}] + \hat{H}'' \quad (14)$$

where we have included the interaction term \hat{H}'' , which is quadratic in the field in the original Hamiltonian (3).

Now we can explicitly introduce the expression for $u^{(4)}$ corresponding to contribution I. Using the standard technique for calculating the reaction of the system to external influences,¹⁸ we find

$$u^{(4)} = - \int_{-\infty}^{\infty} \langle\langle H^{(2)}(t) H^{(2)}(t') \rangle\rangle dt' \quad (15)$$

where

$$\begin{aligned} \langle\langle X(t) Y(t') \rangle\rangle &\equiv \theta(t-t') \cdot \frac{1}{i\hbar} \langle [X(t), Y(t')] \rangle_0 \\ &\equiv \frac{1}{2\pi} \int_{-\infty}^{\infty} \langle\langle X|Y \rangle\rangle_{\nu} e^{-i\nu(t-t')} d\nu \quad (16) \end{aligned}$$

is the retarded two-time Green's function.

We now turn to consideration of the effective Hamiltonian (14). We use it to treat electron transitions from the conduction band c through virtual states in the valence band v : $c_{\alpha} \rightarrow v_{\alpha'} \rightarrow c_{\beta}$, where α and β are spin indices. These transitions can be accompanied by electron spin flip due to spin-orbit interaction, which plays an important role in many conductors, among them A_3B_5 , in determining the top of the valence band. In the Kane model the Hamiltonian can be expressed in terms of the band structure parameters E_g , m_c , and the magnitude of the spin-orbit splitting Δ_{SO} at the top of the valence band. We thus have

$$H_{cc}^{(2)} = \frac{e^2 F^{(1)} F^{(2)}}{m\omega_1\omega_2} \{A_c(\mathbf{e}_1\mathbf{e}_2)\rho_{\mathbf{q}}^{(+)} + iB_c(\mathbf{e}_1\mathbf{e}_2)\rho_{\mathbf{q}}^{(-)}\} \quad (17)$$

where $\mathbf{q} = \kappa_{\omega_1} + \kappa_{\omega_2}$ is the sum of the wave vectors and we have written $\rho_{\mathbf{q}}^{(\pm)} = \rho_{\mathbf{q},1/2} \pm \rho_{\mathbf{q},-1/2}$; $\rho_{\mathbf{q},1/2}$, $\rho_{\mathbf{q},-1/2}$ are the electron density operators with spin projections $\pm 1/2$ in the direction $(\mathbf{e}_1\mathbf{e}_2)$; $F^{(1)}$, $F^{(2)}$ are the electric field strengths; \mathbf{e}_i , \mathbf{e}_j are the unit vectors of the light wave polarization with frequencies ω_i and ω_j . In our case each of these frequencies can assume the values $\pm\omega$, $\pm\Omega$. The coefficients A_c and B_c have the following form:

$$\begin{aligned} A_c &= 1 + \mathcal{P} [2E_g E_{g1}^{-2} - (E_g + \Delta_{\text{SO}}) E_s^{-2}], \\ B_c &= \mathcal{P} [E_{g1}^{-2} - E_s^{-2}], \quad (18) \end{aligned}$$

where

$$\begin{aligned} \mathcal{P} &= (m_c^{-1} - m^{-1}) \frac{E_g(E_g + \Delta_{\text{SO}})}{3E_g + 2\Delta_{\text{SO}}}, \quad E_{g1}^2 = E_g^2 - (\hbar\omega_1)^2, \\ E_s^2 &= (E_g + \Delta_{\text{SO}})^2 - (\hbar\omega_1)^2. \quad (19) \end{aligned}$$

The second terms in the square brackets in (18) are associated with the spin-orbit interaction. In particular, we have $B_c = 0$ at $\Delta_{\text{SO}} = 0$.

A Hamiltonian of the form (17) has been used in many treatments of Raman scattering of light in semiconductors (see Ref. 14).

3. CALCULATION OF THE INDUCED ROTATION OF THE POLARIZATION

To derive $u^{(4)}$ and the corresponding components of the tensor $\chi^{(3)}$ we must calculate the Green's function on the right-hand side of (15). In analogy with Hamilton and McWhorter,¹⁵ who used Eqs. (16)–(19), we write

$$\begin{aligned} \langle\langle H_{cc}^{(2)} | H_{cc}^{(2)} \rangle\rangle_{\nu} &= \frac{e^4 F^{(1)} F^{(2)} F^{(3)} F^{(4)}}{m^2 \omega_1 \omega_2 \omega_3 \omega_4} \\ &\times \sum_{\mathbf{p}, \alpha, \beta} \gamma_{\alpha\beta}^{+(1,2)}(\mathbf{p}) g_{\alpha\beta}^{(3,4)}(\mathbf{p}, \nu), \quad (20) \end{aligned}$$

where

$$\gamma_{\alpha\beta}^{(i,j)} = (\mathbf{e}_i \mathbf{e}_j) A_c \delta_{\alpha\beta} + i B_c \sigma_{\alpha\beta}(\mathbf{e}_i \mathbf{e}_j), \quad (21)$$

$$\begin{aligned} g_{\alpha\beta}^{(3,4)}(\nu) &= -i \int_0^{\infty} e^{i\nu t} \left\langle \left[a_{\mathbf{p},\beta}^+(t) a_{\mathbf{p}+\mathbf{q},\alpha} \right. \right. \\ &\left. \left. \times \sum_{\mathbf{p}', \alpha', \beta'} \gamma_{\alpha'\beta'}^{(3,4)} a_{\mathbf{p}'+\mathbf{q},\alpha'}^+ a_{\mathbf{p}',\beta'} \right] \right\rangle. \quad (22) \end{aligned}$$

Equations (17)–(22) are written using the basis functions $|S, 1/2\rangle$, $|S, -1/2\rangle$ of the conduction band. However, we can no longer put off treating the spin splitting of the conduction band by the perturbation which is cubic in the electron momentum p :

$$\begin{aligned} H_s &= \Omega_{oF} \left(\frac{p}{p_F} \right)^3 \bar{\mathbf{k}} \boldsymbol{\sigma}, \quad \bar{\kappa}_{\mu} = n_{\mu} (n_{\mu+1}^2 - n_{\mu+2}^2), \\ n_{\mu} &= p_{\mu} / p, \quad (23) \end{aligned}$$

where p_F is the bounding Fermi momentum for electrons in the conduction band and Ω_{oF} determines the inverse spin relaxation time for the so-called precession mechanism (see Refs. 20 and 21). An explicit expression for Ω_{oF} will be given below [see Eq. (52)]. Despite the small value of the splitting produced by the operator H_s , it substantially changes the form of the Green's functions (20)–(22), which in the final analysis qualitatively changes the OFE pattern. Taking H_s into account, we can write the new basis functions for the conduction band in the form

$$\begin{aligned} |S_1\rangle &= \exp\left(i \frac{\Phi}{2}\right) \cos \frac{\Theta}{2} |S, \frac{1}{2}\rangle + \exp\left(-i \frac{\Phi}{2}\right) \sin \frac{\Theta}{2} |S, -\frac{1}{2}\rangle, \\ |S_2\rangle &= -\exp\left(i \frac{\Phi}{2}\right) \sin \frac{\Theta}{2} |S, \frac{1}{2}\rangle \\ &+ \exp\left(-i \frac{\Phi}{2}\right) \cos \frac{\Theta}{2} |S, -\frac{1}{2}\rangle. \quad (24) \end{aligned}$$

In the system of coordinates with z axis parallel to $\mathbf{e}_1\mathbf{e}_2$, only the z component of the Pauli matrix remains in Eq. (21). In the new basis we have

$$\vec{\sigma}_z = \begin{pmatrix} \cos \Theta & e^{-i\Phi} \sin \Theta \\ e^{i\Phi} \sin \Theta & -\cos \Theta \end{pmatrix}. \quad (25)$$

In (24) and (25) we have used the notation

$$\Phi = \arctan \frac{\tilde{\kappa}_y}{\tilde{\kappa}_x}, \quad \cos \Theta = \frac{\tilde{\kappa}_z}{|\tilde{\kappa}|}, \quad \sin \Theta = \frac{\sqrt{\tilde{\kappa}_x^2 + \tilde{\kappa}_y^2}}{|\tilde{\kappa}|}. \quad (26)$$

The expressions that follow will be written in the basis (24).

Let us find the equations of motion for the quantities $g_{\alpha\beta}(\mathbf{p}, \nu)$. To describe the effects of screening of density fluctuations systematically it is necessary to take into account the interelectron Coulomb interaction and the interaction between electrons and longitudinal optical phonons, which changes the effective interelectron interaction. The latter effect is described by the dielectric function

$$\varepsilon(\omega) = \varepsilon_\omega \left(1 + \frac{\Omega_l^2 - \Omega_t^2}{\Omega_l^2 - \omega^2} \right), \quad (27)$$

where Ω_l and Ω_t are the frequencies of the longitudinal and transverse oscillations of the optical phonons ($\Omega_t^2 = \Omega_l^2 \varepsilon_\infty / \varepsilon_0$). We write the corresponding electron-phonon Hamiltonian in the form

$$\begin{aligned} \kappa_c = & \sum_{\mathbf{k}, \sigma} \mathcal{E}_{\mathbf{k}\sigma} a_{\mathbf{k}\sigma}^+ a_{\mathbf{k}\sigma} \\ & + \frac{1}{2} \sum_{\mathbf{q}} \frac{4\pi e^2}{q^2 \varepsilon_\infty} \sum_{\mathbf{k}, \sigma} a_{\mathbf{k}+\mathbf{q}, \sigma}^+ a_{\mathbf{k}'-\mathbf{q}, \sigma'}^+ a_{\mathbf{k}', \sigma'} a_{\mathbf{k}, \sigma} \\ & + \hbar \Omega_1 \sum_{\mathbf{q}} \zeta_{\mathbf{q}}^+ \zeta_{\mathbf{q}} - ie(2\pi\hbar\Omega_l)^{1/2} (\varepsilon_\infty^{-1} - \varepsilon_0^{-1}) \\ & \times \sum_{\mathbf{k}, \mathbf{q}, \sigma} q^{-1} (\zeta_{\mathbf{q}} - \zeta_{-\mathbf{q}}^+) a_{\mathbf{k}+\mathbf{q}, \sigma}^+ a_{\mathbf{k}, \sigma}, \end{aligned} \quad (28)$$

where $\zeta_{\mathbf{q}}^+$, $\zeta_{\mathbf{q}}$ are creation and annihilation operators for longitudinal optical phonons; the index σ labels the subbands of the conduction band c split with respect to spin.

Strictly speaking, the second and fourth terms on the right-hand side of (28), which were introduced to describe the Coulomb and electron-phonon interactions, should be subjected to the transformation (7)–(9) just like the Hamiltonian (3). In the transformed Hamiltonian and in the expression for the internal energy, additional terms of all orders in the field of the electromagnetic wave then appear, including the Coulomb and electron-phonon interaction. We will not take into account these corrections to the quantities calculated here, assuming instead that

$$\frac{e^2}{\varepsilon_0 \hbar v_F} = \frac{e^2 m_c}{(3\pi^2)^{1/3} \hbar \varepsilon_0 n_0^{1/3}} \ll 1, \quad (29)$$

and that electron-phonon coupling is weak. For materials like InSb or InAs, Eq. (29) is satisfied at free-electron densities $n_0 \geq 10^{17} \text{ cm}^{-3}$. Furthermore, terms describing “spin flip” (here we are talking about the projection of the spin in

the direction $\tilde{\kappa}$) should be added to the second and fourth terms on the right-hand side of (28). However, these corrections contain the factor

$$\frac{1}{V} \int u_{\sigma, \mathbf{k} + \mathbf{q}}^* u_{\sigma', \mathbf{k}} dr,$$

where $u_{\sigma, \mathbf{k}}$ are the Bloch amplitudes. This factor differs significantly from $\delta_{\sigma\sigma'}$ only at large values of q ; these are unimportant in the present case.

Using the Hamiltonian (28) we find equations of motion for $g_{\alpha\beta}$ in the usual manner in the random phase approximation (see, e.g., Ref. 22, Ch. 3). After Fourier transforming we find

$$\begin{aligned} & [\nu - \omega_{\alpha\beta} - \mathbf{q}\mathbf{v} + i\tau_s^{-1}(1 - \delta_{\alpha\beta})] g_{\alpha\beta}(\mathbf{k}, \nu) \\ & = \gamma_{\alpha\beta}(\nu + \mathbf{q}\mathbf{v}) \left(-\frac{\partial f}{\partial \mathcal{E}} \right) + \delta_{\alpha\beta} \frac{4\pi e^2}{q^2 \varepsilon(\nu)} (\omega_{\alpha\beta} + \mathbf{q}\mathbf{v}) \\ & \quad \times \sum_{\mathbf{k}', \sigma} g_{\sigma\sigma}(\mathbf{k}', \nu) - i\tau_p^{-1} \left[g_{\alpha\beta}(\mathbf{k}', \nu) \right. \\ & \quad \left. - \int \frac{d\Omega_{\mathbf{k}}}{4\pi} g_{\alpha\beta}(\mathbf{k}', \nu) \right], \end{aligned} \quad (30)$$

where $f(\mathcal{E})$ is the electron distribution function in the c band. The integration in the last term on the right-hand side of (30) is performed over solid angles in \mathbf{k} space. In Eq. (30) we have introduced the spin relaxation time τ_s and the relaxation time τ_p for the electron momentum.

We introduce the notation

$$\begin{aligned} \Omega_{\alpha\beta} &= \omega_{\alpha\beta} + \mathbf{q}\mathbf{v}, \quad \tau_{\alpha\beta}^{-1} = \tau_p^{-1} + \tau_s^{-1}(1 - \delta_{\alpha\beta}), \\ \omega_{\alpha\beta} &= \left(\frac{p}{p_F} \right)^3 |\tilde{\kappa}| (\delta_{\alpha 1} \delta_{\beta 2} - \delta_{\beta 1} \delta_{\alpha 2}), \\ \nu_{\mathbf{q}} &= \nu - \mathbf{q}\mathbf{v} + i\tau_p^{-1}, \quad \nu_{\alpha\beta} = \nu - \Omega_{\alpha\beta} + i\tau_{\alpha\beta}^{-1}. \end{aligned} \quad (31)$$

Solving (30) we find

$$\begin{aligned} \sum_{\mathbf{k}, \alpha, \beta} \gamma_{\alpha\beta}^{+(1,2)} g_{\alpha\beta}^{(3,4)}(\mathbf{k}, \nu) &= - \left[\mathcal{L}_2 - \frac{4\pi e^2}{q^2} \frac{\mathcal{L}_1^2}{\varepsilon_l(\mathbf{q}, \nu)} \right] \\ & \quad \times (\mathbf{e}_1 \mathbf{e}_2)(\mathbf{e}_3 \mathbf{e}_4) \\ & \quad - \mathcal{K}(\mathbf{e}_1 \mathbf{e}_2)(\mathbf{e}_3 \mathbf{e}_4), \end{aligned} \quad (32)$$

$$\begin{aligned} \mathcal{L}_j &= \frac{2}{(2\pi\hbar)^3} \int d^3 k A_c^j \frac{\mathbf{q}\mathbf{v}(\partial f / \partial \mathcal{E})}{\nu_{\mathbf{q}} [1 - i\tau_p^{-1} \langle \nu_{\mathbf{q}}^{-1} \rangle]}, \\ \mathcal{K} &= \frac{1}{(2\pi\hbar)^3} \int d^3 k B_c^2 \left(\frac{\partial f}{\partial \mathcal{E}} \right) \tilde{\mathcal{K}}_{\kappa}, \end{aligned} \quad (33)$$

where $\langle \dots \rangle$ represents averaging over angle and

$$\tilde{\mathcal{K}}_{\kappa} = \frac{1}{|\kappa|^2} \sum_{\alpha, \beta=1}^2 \tilde{\mathcal{K}}_{\alpha\beta} [\tilde{\kappa}_z^2 \delta_{\alpha\beta} + (\tilde{\kappa}_x^2 + \tilde{\kappa}_y^2)(1 - \delta_{\alpha\beta})], \quad (34)$$

$$\tilde{\mathcal{K}}_{\alpha\beta} = \Omega_{\alpha\beta} \nu_{\alpha\beta} [1 - i\tau_p^{-1} \langle \nu_{\alpha\beta}^{-1} \rangle]^{-1},$$

$$\varepsilon_l(\mathbf{q}, \nu) = \varepsilon(\nu) + \frac{4\pi e^2}{q^2} \mathcal{L}_0. \quad (35)$$

Note that the first term on the right-hand side of (32), which describes electron density fluctuations, does not depend on the spin splitting of the conduction band. The latter enters only into the second term of (32), associated with spin-density fluctuations. It is very significant that, as can be seen from (32) this term, unlike the first, is not suppressed by Coulomb shielding. This result is of course a consequence of the fact that the spin-density fluctuations do not carry electric charge.

When the frequencies Ω and ω of the probe and pump radiation are nearly equal and propagate nearly parallel, the frequency differences ν and the differences in the wave vectors q are such that

$$\nu, qv_F \ll \tau_p^{-1}. \quad (36)$$

As a rule we have

$$\Omega_{oF}, \tau_s^{-1} \ll \tau_p^{-1}.$$

For convenience in the notation below we introduce the quantities $\Omega_{\alpha\beta}$ and $\tilde{\tau}_{\alpha\beta}$, defined by

$$(\nu - \Omega'_{\alpha\beta} + i\tilde{\tau}_{\alpha\beta}^{-1})^{-1} \equiv \langle (\nu - \Omega_{\alpha\beta} + i\tau_{\alpha\beta}^{-1})^{-1} \rangle. \quad (37)$$

To within terms of second order in $\Omega_{\alpha\beta}\tau_p$ we have

$$\begin{aligned} X &\equiv \nu - \langle \Omega_{\alpha\beta} \rangle = \nu_1 (1 - \tau_{\alpha\beta}^2 \nu_2^2)^{-2}, \\ \tilde{\tau}_{\alpha\beta} &= \tau_{\alpha\beta}^2 (1 - \tau_{\alpha\beta}^2 \nu_2^2), \end{aligned} \quad (38)$$

where

$$\nu_1 = \nu - \langle \Omega_{\alpha\beta} \rangle, \quad \nu_2^2 = \langle (\nu - \Omega_{\alpha\beta})^2 \rangle.$$

More detailed analysis reveals that $X|_{\nu\tau_p^{-1}} \sim \tau_p^{-1}$. Then we have

$$\begin{aligned} \text{Re } \tilde{\mathcal{K}}_{\alpha\beta} &\left\{ \begin{aligned} &= \frac{\Omega_{\alpha\beta}}{(\tilde{\mathcal{T}}_{\alpha\beta}^{(1)})^2 + (\tilde{\mathcal{T}}_{\alpha\beta})^2} \\ &\times \left[\begin{aligned} &[(\nu - \Omega'_{\alpha\beta}) \tilde{\mathcal{T}}_{\alpha\beta}^{(1)} + \tilde{\tau}_{\alpha\beta}^{-1} \tilde{\mathcal{T}}_{\alpha\beta}] \\ &[(\Omega'_{\alpha\beta} - \nu) \tilde{\mathcal{T}}_{\alpha\beta} + \tilde{\tau}_{\alpha\beta}^{-1} \tilde{\mathcal{T}}_{\alpha\beta}^{(1)}] \end{aligned} \right] \end{aligned} \right. \quad (39) \end{aligned}$$

where

$$\begin{aligned} \tilde{\mathcal{T}}_{\alpha\beta} &= \tilde{\tau}_{s\alpha\beta}^{-1} (\nu - \Omega_{\alpha\beta}) + \tau_{\alpha\beta}^{-1} (\nu - \Omega'_{\alpha\beta}), \\ \tilde{\mathcal{T}}_{\alpha\beta}^{(1)} &= (\nu - \Omega_{\alpha\beta}) (\nu - \Omega'_{\alpha\beta}) - \tau_{\alpha\beta}^{-1} \tau_{s\alpha\beta}^{-1}, \\ \tilde{\tau}_{s\alpha\beta}^{-1} &= \tilde{\tau}_{\alpha\beta}^{-1} - \tau_p^{-1}. \end{aligned} \quad (40)$$

Since $\tilde{\tau}_s^{-1}$ is smaller than the other quantities of the same dimensionality, when the ‘‘hydrodynamic’’ conditions (36) hold we find

$$\begin{aligned} \text{Re } \tilde{\mathcal{K}}_{\alpha\beta} &\approx \frac{\Omega_{\alpha\beta} \tilde{\tau}_{\alpha\beta}^{-1} \tau_{\alpha\beta}^{-1}}{\tau_{\alpha\beta}^{-2} (\nu - \Omega'_{\alpha\beta})} \approx \frac{\omega_{\alpha\beta} + \mathbf{q}\mathbf{v}}{\nu - \langle \omega_{\alpha\beta} \rangle}, \\ \text{Im } \tilde{\mathcal{K}}_{\alpha\beta} &\approx \tau_{\alpha\beta} \Omega_{\alpha\beta} \frac{\Omega_{\alpha\beta} - \Omega'_{\alpha\beta}}{\nu - \Omega'_{\alpha\beta}} \ll \text{Re } \tilde{\mathcal{K}}_{\alpha\beta}. \end{aligned} \quad (41)$$

Equations (20)–(22), (32)–(35), and (39)–(41) determine the internal energy $u^{(4)}$ of the electron system in the field of the light waves. The components of the cubic sus-

ceptibility tensor $\chi^{(3)}$ are found by differentiating $u^{(4)}$ four times with respect to the Cartesian components $F^{(i)}$ of the fields whose frequencies ω_i assume the values $\pm\omega, \pm\Omega$. In evaluating the differences in the components of the susceptibilities $\chi^{(a)}$ determining the magnitude $\bar{\theta}$ of the OFE, we will assume for simplicity that the distribution function $f(\mathcal{E})$ is a Fermi step function. Since we have in mind the interpretation of experiments performed at 300 K or 90 K, this requires explanation. Because of the small effective masses and high (10^{17} – 10^{18} cm $^{-3}$) densities n_0 under experimental conditions, the electron gas is at least partly degenerate. In this case the approximation of $f(\mathcal{E})$ by a step function yields reasonable estimates for the parameters of the problem. On the other hand, as long as we can only contemplate qualitative comparison between theory and experiment, the extraordinarily difficult analysis of the temperature dependence of the OFE is not justified.

We find

$$\bar{\theta} = \frac{\pi}{16\Omega} \left[\frac{e q_{FT}}{m c \omega \kappa_0(\Omega)} \right]^2 \sum_{i,j=1}^2 r_i r_j \tilde{\theta}(r_i \Omega, r_j \omega), \quad (42)$$

where q_{FT}^{-1} is the Thomas–Fermi shielding radius, we have written $r_i \equiv (-1)^i$, and

$$\begin{aligned} \tilde{\theta}(\Omega, \omega) &= 8B_c(\omega)B_c(\Omega) \mathcal{K}(\Delta\omega, \Delta\mathbf{q}_\omega) + \sum_{i=1}^2 [B_c(\omega) \\ &+ r_i B_c(\Omega)]^2 \mathcal{K}(\Omega - r_i \omega, \kappa_\Omega - r_i \kappa_\omega), \end{aligned} \quad (43)$$

$$\mathcal{K}(\nu, \mathbf{q}) = \langle \tilde{\mathcal{K}}_{\kappa}(\nu, \mathbf{q}) \rangle.$$

The quantities $\mathcal{K}_{\alpha\beta}$ are given by Eqs. (39), where now $\nu = \nu_F, p = p_F$ [see the definition (31)]. It should be kept in mind that the spin splitting of the conduction band at the Fermi level satisfies $\Omega_{oF} \propto n_0, \nu_F \propto n_0^{1/3}$. Here $\Delta\omega$ and $\Delta\mathbf{q}_\omega$ in Eq. (43) stand for differences in frequency and wave vector among the various lines of the pump radiation spectrum. Let us clarify this somewhat. The experiments which will be described below in Sec. 4 were performed with probe and pump radiation including either several lines of the rotational spectrum of the laser radiation or a single line (actually each of these lines itself has line structure consisting of longitudinal–transverse laser radiation modes).

In the case of a ‘‘comb’’ of almost equidistant lines, the rotational contribution to the observed effect comes from all possible four-wave processes of the form $\Omega_r = \omega_r - \omega_s + \Omega_s$. If we take into account the phases of the individual rotational lines, the expression for $\tilde{\mathcal{K}}_{\kappa}$ in Eq. (43) is replaced by

$$\begin{aligned} \tilde{\mathcal{K}}_{\kappa}^{\prime} &= \sum_{r,s,t} \beta_r \beta_{r+t} \beta_s \beta_{s+t} \tilde{\mathcal{K}}_{\alpha\beta}(t\Delta\omega_1) \\ &\times \exp[i(\varphi_r^\Omega - \varphi_{r+t}^\Omega - \varphi_s^\omega + \varphi_{s+t}^\omega)], \end{aligned} \quad (44)$$

where β_r is the relative intensity of the r th rotational line.

Next we will consider both Raman contributions to \mathcal{K} and contributions of the individual rotational lines. We will also distinguish between intra- and interbranch components ($\alpha = \beta$ and $\alpha \neq \beta$), where the intermediate virtual states

(which the electron reaches under the action of the perturbation $\tilde{H}_{cc}^{(2)}$) are in the same spin branch as the initial state or in a different branch.

We begin by considering the intrabranh components. For them we easily find

$$\operatorname{Re} \tilde{\mathcal{H}}_{\alpha\alpha} \approx \frac{\tau_p^2 s^2}{3} \frac{(\tilde{\omega}^2 + \frac{1}{3}s^2)}{\tilde{\omega}^2 + (\tilde{\omega}^2 + \frac{1}{3}s^2)\tau_p^2}, \quad s = |(\mathbf{q}\mathbf{v})|. \quad (45)$$

Suppose all lines are rotational. The laser radiation spectrum consists of l narrow (width $\delta\nu \ll s$) components with relative intensities $\tilde{\beta}_i$. Assuming for simplicity that they have the same phases, we find

$$\tilde{\theta} \propto \sum_t \left(\sum_{i=1}^l \tilde{\beta}_i \tilde{\beta}_{i+t} \right)^2 \chi^{(a)}(t\Delta\tilde{\omega}_1). \quad (46)$$

If we look at the simplest case, in which $\tilde{\beta}_i = i^{-1/2}$ holds for all i , then we have

$$\sum_i \tilde{\beta}_i \tilde{\beta}_{i+t} = (l-t)/t.$$

Hence

$$\chi^{(a)} = \chi^{(a)}(0) + 2 \sum_t \left(\frac{l-t}{t} \right)^2 \chi^{(a)}(t\Delta\tilde{\omega}_1), \quad (47)$$

where we can use (45) to calculate $\chi^{(a)}$. For $s \gg \delta\nu$, the quantity $\chi^{(a)}(0)$ does not depend on density. As n_0 increases, the magnitude of the OFE grows because $\chi^{(a)}(t\Delta\tilde{\omega}_1)$ contributes significantly to (47) with larger and larger values of t .

For Raman contributions the intrabranh component is small, so that in this case we have $\tilde{\omega} \gg s/3$, $\tilde{\omega}\tau_p < 1$, $\operatorname{Re} \tilde{\mathcal{H}}_{\alpha\alpha} \approx \tau_p^2 s^2/3 \ll 1$.

Now consider interbranch components. In the case of a single rotational line we have

$$\operatorname{Re} \tilde{\mathcal{H}}_{12}|_{1l} \approx \frac{\Omega_{12}}{\Omega_{0F}} (1-\eta) \left[1 + \frac{\langle \Omega_{0F} \rangle}{\langle \Omega_{0F} \rangle^2} \gamma (1-\eta)^2 \times (1+a^2)\eta \right]^{-1}, \quad (48)$$

$$\eta \equiv \tau_{12}^2 \langle \Omega_{0F}^2 \rangle,$$

where γ is a numerical factor ($\gamma \leq 1$); a enters into the expression for the spin relaxation time according to Ref. 20 $\tau_s^{-2} = a^2 \eta$, which can also be written in the form

$$\tau_s^{-1} = a \tau_p (16/35) \tilde{\alpha}^2 E_F^2 / (\hbar^2 E_g), \quad (49)$$

$$\tilde{\alpha} = 4 \Delta_{SO} m_{cv}^{-1} [(E_g + \Delta_{SO})(3E_g + 2\Delta_{SO})]^{-1/2},$$

$$m_{cv} \approx 0.8m. \quad (50)$$

The value of a in Eq. (49) depends on the scattering behavior of the carriers. For example, for scattering on charged impurities in the case of the degenerate electron gas we have $a \approx 1/9$ (Ref. 20), while for a nondegenerate gas we have $a \approx 105/32$ (Ref. 21). Equation (48) is correct for values of n_0 that are not too small, such that $\Omega_{0F} \gg \nu_F q$. If η is not

very small, then $|\operatorname{Re} \tilde{\mathcal{H}}_{12}|$ is much less than unity. Thus, in the case in which both probe and pump radiation consists of a single line of the laser rotational spectrum the interbranch component dominates. The intrabranh component has the opposite sign, and as can be seen from (48) decreases in magnitude as n_0 grows, which causes the induced rotation angle to increase.

Let us now consider the intrabranh component of the Raman contribution to OFE. Under the conditions of the present experiments (see Sec. 4) the main contribution to $\tilde{\mathcal{H}}(\nu, q)$ comes from the interaction between neighboring rotational lines. Then in the argument of $\tilde{\mathcal{H}}$ their frequency difference $\pm \Delta\omega_1$ appears and

$$\operatorname{Re} \tilde{\mathcal{H}} \approx \frac{2}{3} \frac{\langle \Omega_{0F} \rangle}{\Delta\omega_1 - \langle \Omega_{0F} \rangle}. \quad (51)$$

In our experiment $\Delta\omega_1 \approx 3.7 \cdot 10^{11} \text{ s}^{-1}$. An estimate yields

$$\langle \Omega_{0F} \rangle = |\langle \tilde{\alpha} (2m_c E_g^{-1/2}) | \tilde{k} | (p_F/p)^3 \rangle| \sim 10^{11} \text{ s}^{-1} \cdot (n_0 \cdot 10^{-17} \text{ cm}^3). \quad (52)$$

Thus, for $n_0 \geq 10^{17} \text{ cm}^{-3}$ we can expect $\tilde{\theta}(n_0)$ to increase sharply as the spin splitting of the conduction band at the Fermi level $\langle \Omega_{0F} \rangle \propto n_0$ approaches the difference in frequencies of neighboring laser lines.

The simple formula (51) holds for $\Delta\omega_1 - \langle \Omega_{0F} \rangle \gg \tau_s^{-1}$. To describe the resonant region expression (39) should be used.

4. EXPERIMENTAL TECHNIQUE

To study the optical Faraday effect in n -type InAs and InSb we used a CO₂ laser with a continuous longitudinal discharge and a Q -switched resonator. The pulses had a maximum power of $\sim 10 \text{ kW}$ and a length of 10^{-7} s ; the repetition rate was $\sim 5 \cdot 10^{-2} \text{ pulses s}$. A diffraction grating ($\sim 100 \text{ lines/mm}$) or an aluminized mirror was used as one element of the laser cavity. Thus in various experiments we used either spectrally unresolved radiation, consisting of eight approximately equidistant narrow lines of the rotational spectrum in the 10.6 or 9.5 μm band, or a single spectral component with width less than 10^9 s^{-1} was generated.

Part ($\sim 2\%$) of the basic laser beam was split off and directed by the mirror at the slit of an IKM-1 grating monochromator ($\sim 100 \text{ lines/mm}$) in order to monitor the spectral composition of the light. Then the laser beam was split into two beams, one of which (the weaker) was used as the probe radiation, while the other was used as the pump. The two beams could be focused on the sample from either direction at a small angle with respect to one another. In the sample the angle between the beams was less than 1.5° . The beams were mixed in the sample using a small diaphragm (diameter 300 μm) fastened directly to the sample on the pump side. The pump could be focused on the sample in such a way that the diaphragm stopped all but the central part of the beam (at the level 0.7 of the maximum value of the intensity). The probe radiation was focused more sharply and almost coaxially with the pump. Consequently the probe passed through

the region of the sample where the pump was propagating relatively uniformly, and did not experience much diffraction after passing through the diaphragm.

Samples of n -InAs were cleaved in the form of thin wedges with an angle $\sim 3^\circ$. They varied in thickness, depending on the density n_0 of the free carriers so that $\alpha d \leq 1.3$. The samples were fixed in the opening of the cold pipe of a vacuum nitrogen cryostat with windows made of BaF_2 .

Along the path of the pump radiation in front of the lens that focused the radiation onto the sample, a quarter-wave plate of CdS was fastened, which transformed the linearly polarized laser radiation into circularly polarized radiation. After passing through the diaphragm and the sample, the beam was deflected by a small mirror to a photodetector used as a monitor.

The probe radiation was linearly polarized. Its intensity at the sample was less than 3% of the pump intensity. After the sample in front of the photodetector along the path of the probe radiation an analyzer with polarization ratio $1/4 \cdot 10^4$ was placed. The analyzer was fastened to a special worm gearing. This allowed us to measure very small rotation angles of the polarization plane of the probe radiation, and also to detect a small induced ellipticity or depolarization.

In some experiments the probe radiation, after passing through the sample and analyzer, was directed to a monochromator and then to the photodetector. Thus, for the unresolved probe radiation we could measure the rotation angle induced by the pump for each of the spectral components of the probe. In some experiments we used the second harmonic of the split beam ($\lambda \approx 5.3$ or $4.75 \mu\text{m}$) as the probe. In this case a tellurium crystal was placed in the probe radiation channel, while the primary radiation was filtered out by a sapphire plate located right at the probe photodetector. The photodetectors were made from cooled "Svod" photoresistors. The load and hence the time constant τ_{ph} of the probe photodetectors were chosen so as to integrate possible intermode beats resulting from four-wave interactions of the individual longitudinal—transverse modes of the laser radiation ($\tau_{\text{ph}} \sim 4 \cdot 10^{-7}$ s).

To reduce the effect of the light scattered from the pump radiation in the probe measurement channel, and also to simplify detection of the signal, the sequence of pulses was modulated by a chopper with frequency ~ 25 Hz in front of the sample. The modulated sequence of electrical pulses from the photodetector was synchronously demodulated with a $5 \cdot 10^{-8}$ s strobe, and their envelope was resolved using a reference pulse from the monitoring photodetector. Then the envelope was amplified and the first harmonic was extracted and fed to a phase detector, the reference signal to which came from the modulator. The resulting signal was recorded.

For each sample we measured the intensity of the probe radiation that passed through the analyzer as a function of the analyzer rotation angle $\tilde{\varphi}$ for left and right circularly polarized pump radiation and measured the angle θ through which the plane of polarization of the probe radiation rotated. The intensity of the pump radiation was chosen in each case so that there was almost no nonlinear absorption of the

pump radiation or amplitude modulation of the probe. This meant that the probe radiation was weaker.

From the measured value of the angle θ and the probe absorption coefficient α we determined the coefficient of the cubic nonlinearity $\chi^{(3)}$ responsible for the OFE [see Eqs. (1) and (2)].

In our experiments we studied the density dependence of $\chi^{(a)}$ in n -InAs and n -InSb samples under various conditions. Since some of the available InAs samples were nonuniform, we measured the transmissivity T at a large number of points on one level and found the function $\ln T(d_i)$. In fairly uniform samples these curves were straight lines whose slope determined the value of $\alpha(\omega)$.

The values of the intensity I_ω were found by measuring the pump radiation flux with a calibrated photoresistor with a large sensitive area immediately behind the diaphragm with no sample, and dividing this flux by the area of the diaphragm. The resulting values of $\chi^{(a)}$ for each sample were correlated with the densities n_0 found from Hall measurements.

5. EXPERIMENTAL RESULTS AND DISCUSSION

As shown by the experiments, the results of which are given below, angles through which the polarization plane of the probe rotated are quite large: $\sim 10^2$ deg·cm/MW for InAs and $\sim 10^3$ deg·cm/MW for InSb. In this connection we should discuss the possible contribution to the observed photoinduced polarization rotation of the processes mentioned in the Introduction, associated with the spin orientation of the carriers by the pump radiation. Since the measurements were performed in n -type samples, the effects associated with inter-subband transitions between complex valence bands, observed previously in Ref. 13, were negligible here on account of the low hole density. The electrons in InSb can in principle undergo spin orientation under the action of the radiation from the CO_2 laser due to two-photon interband transitions. This process was studied theoretically and experimentally in Ref. 23. It was found that, at least for $T \geq 80$ K, no actual spin orientation occurs in InSb, which is a consequence of the short spin relaxation time. The contribution of the spin orientation mechanism due to indirect transitions involving phonons between conduction bands through virtual states in the valence band was also evaluated. This contribution was found to be small in comparison with the observed magnitude of the effects and with the contribution of the spin-density fluctuation mechanism calculated above. Estimates of the polarization rotation of the probe radiation due to effects associated with spin splitting of the conduction band by the pump radiation gives rise to rotation angles an order of magnitude smaller than for the spin-density fluctuation mechanism.

The experiments revealed that the density dependence of $\chi^{(a)}$ varies in cases when the spectral composition of both beams (with ω close to Ω) includes a "comb" of rotational lines and when there is only one spectral component. The role of the Raman contributions emerges in the spectral dependence of the polarization rotation angle θ , which was found as follows. The probe and pump radiation were directed at the sample in the form of spectrally unresolved

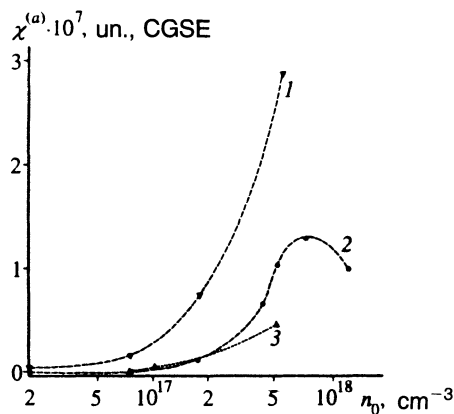


FIG. 1. Dependence of $\chi^{(a)}$ on n_0 in n -InAs. The pump and probe spectra consist of a set of rotational lines; 1, 2) pump and probe radiation propagating in the same direction: 1) $T=90$ K; 2) $T=300$ K; 3) pump and probe radiation propagating antiparallel, $T=300$ K.

light beams containing eight rotational lines each. After passing through the sample each spectral component was extracted from the probe radiation successively and the rotation of the plane of polarization induced in it was measured. This spectrum was quite complicated. In particular, it contained four sign changes in an interval of 2 meV. Since this spectral behavior was found in p -InAs and p -Ge, we conclude that this type of spectrum is associated not with the microscopic OFE mechanism, which in these materials is related to the phototransitions of holes between subbands of the complex valence band¹³ and is distinctly different from that observed in the present work, but with the distribution of phases of the probe and pump radiation lines as they interact nonlinearly.

The behavior of $\chi^{(a)}(n_0)$ for the case of a comb in "parallel" experimental geometry is shown in Fig. 1 (traces 1 and 2). The rapid growth of $\chi^{(a)}$ for $n_0 > 10^{17}$ cm⁻³ corresponds to the Raman resonance at the transition between spin branches of the conduction band [see Eq. (51)]. At $T=300$ K we could observe the peak described by Eq. (39). Note that the density dependence of $\chi^{(a)}$ found in one line of the rotational spectrum has a different form (Fig. 2).

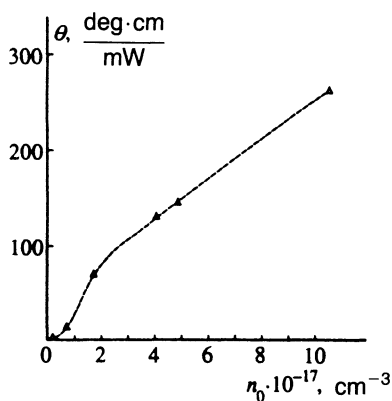


FIG. 2. Angle through which the plane of polarization of the probe radiation rotates as a function of n_0 . The spectrum contains a single rotational line; $T=300$ K.

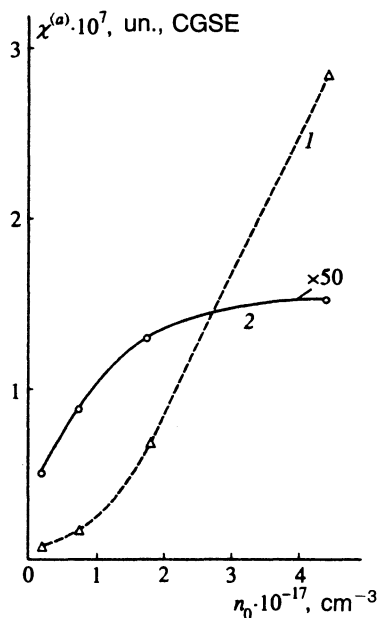


FIG. 3. Dependence of $\chi^{(a)}$ on n_0 in n -InAs for pump and probe radiation having identical and substantially different frequencies: 1) $\hbar\omega=0.117$ eV, $\hbar\omega=0.234$ eV; 2) $\hbar\omega=\hbar\Omega=0.117$ eV. The beams are propagating in the same direction.

In order to explain the density dependence of the OFE in the case of a single rotational spectral component it is necessary to take into account the competition between the intraband component described by Eqs. (45)–(47) and the interband component [Eqs. (48)–(50)]. These components have different signs. The intraband component dominates for large values of n_0 . For small values of n_0 the two contributions are comparable. But the data available at present are inadequate for a quantitative comparison between theory and experiment.

When the probe and pump frequencies are substantially different, as one might expect, no rapid increase in $\chi^{(a)}(n_0)$ is observed for $n_0 > 10^{17}$ cm⁻³ (see Fig. 3, trace 2). In this case the occurrence of the Raman resonance in transitions between the spin branches of the conduction band is naturally excluded.

Measurements have been performed when the pump and probe beams were spectrally unresolvable and when the beams were directed at the sample from opposite sides. It was found that for all samples where measurements were made the quantity $\chi^{(a)}$ is larger for "parallel" experimental geometry than for "antiparallel," and the rate of increase of $\chi^{(a)}$ (Fig. 4) in the latter case was significantly lower.¹⁾ In order to explain this we return to Eq. (43). For the OFE mechanism we are discussing the first term in (43) in the transition to antiparallel geometry does not change, the contribution of the $i=1$ term in the summation for $\Omega \approx \omega$ is vanishingly small [see also Eqs. (34) and (35)], but the $i=2$ term changes not only in magnitude but also in sign. Instead of $\mathbf{q} = \kappa_\Omega - \kappa_\omega$, in the argument of \mathcal{H} now $\mathbf{q}' = \kappa_\Omega + \kappa_\omega \approx 2\kappa_\omega$, appears, with q' two orders of magnitude larger than q under experimental conditions. In this situation a regime develops in which spatial dispersion of the electron plasma occurs to a

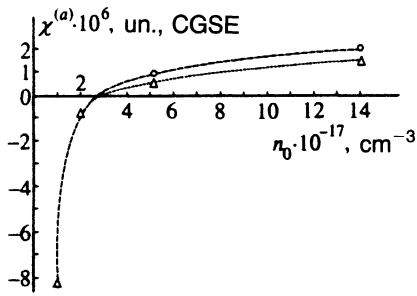


FIG. 4. Dependence of $\chi^{(a)}$ on n_0 for n -InSb: 1) when a single rotational spectral line is present; 2) for unresolved beams. Here $T=300$ K.

marked extent: $q'v_F \approx \tau_p^{-1}$, $\Delta\omega_1$, and all components of \mathcal{R} for Raman processes are close to -1 . In the first term on the right-hand side of (43), however, only the components describing the interaction between neighboring spectral lines are large in comparison with unity. As a result, there are two terms with opposite signs in the right-hand side of (43) which are comparable in magnitude. It is this which is manifested in the observed decrease in the magnitude of the effect.

Until now we have been concerned with the situation in which the spin-density fluctuation mechanism dominated over the whole relevant free-electron density region. Experiments have been performed, however, in which a different OFE mechanism occurred for small values of n_0 , associated with virtual allowed—forbidden electron transitions between the valence band and the conduction band under conditions close to two-photon resonance $\hbar\omega + \hbar\Omega \approx E_g$. In particular, measurements were made in n -InAs with $\hbar\omega=0.131$ eV, $\hbar\Omega=0.262$ eV, and in n -InSb with $\hbar\omega=\hbar\Omega=0.117$ eV. In the first case the interband mechanism and the spin-density fluctuation mechanism yield comparable contributions to the OFE for $n_0 \sim 10^{16}$ cm $^{-3}$, but as n_0 increases the spin-density fluctuation mechanism begins to play the major role. In InSb the interband mechanism dominates for $n_0 \lesssim 2.5 \cdot 10^{17}$ cm $^{-3}$, while at higher densities, such as in InAs, the spin-density fluctuation mechanism is the primary one. The sign of the effect in InSb at large values of n_0 is the same as in InAs (see Fig. 4). The dependence on whether the pump and probe radiation are directed parallel or antiparallel is observed to be

typical of the spin-density fluctuation mechanisms. In the small- n_0 range in InSb this behavior was not observed, which is consistent with the result of theory^{5,7} for the interband OFE mechanism.

¹⁾The different signs of the angles θ for parallel and antiparallel beams in Ref. 12 resulted because in that work the change in the direction of rotation of the polarization of the pump radiation relative to the probe radiation was not taken into account.

- ¹P. W. Atkins and L. D. Barron, *Molec. Phys.* **15**, 503 (1968).
- ²T. Thirunamachandran, *Proc. R. Soc.* **A365**, 327 (1979).
- ³L. P. Rapoport, B. A. Zon, and N. L. Manakov, *Theory of Multiphonon Processes in Atoms* [in Russian], Atomizdat, Moscow (1978).
- ⁴L. D. Landau and E. M. Lifshitz, *Electrodynamics of Continuous Media*, 2nd ed., Pergamon, New York (1984).
- ⁵E. Yu. Perlin, *Fiz. Tverd. Tela* **22**, 66 (1980) [*Sov. Phys. Solid State* **22**, 38 (1980)].
- ⁶A. M. Danishevskii, S. F. Kochegarov, and V. K. Subashiev, *Pis'ma Zh. Eksp. Teor. Fiz.* **33**, 625 (1981) [*JETP Lett.* **33**, 611 (1981)].
- ⁷A. M. Danishevskii and E. Yu. Perlin, *Pis'ma Zh. Eksp. Teor. Fiz.* **41**, 426 (1985) [*JETP Lett.* **41**, 524 (1985)].
- ⁸P. M. Butcher and T. P. McLean, *Proc. Phys. Soc.* **81**, 219 (1963).
- ⁹P. A. Wolff and G. A. Pearson, *Phys. Rev. Lett.* **17**, 1015 (1966).
- ¹⁰K. C. Rustagi, *Phys. Rev.* **B2**, 4053 (1970).
- ¹¹S. Y. Yuen and P. A. Wolff, *Appl. Phys. Lett.* **40**, 457 (1982).
- ¹²A. M. Danishevskii and E. Yu. Perlin, *Pis'ma Zh. Eksp. Teor. Fiz.* **41**, 426 (1985) [*JETP Lett.* **41**, 524 (1985)].
- ¹³A. M. Danishevskii, E. L. Ivchenko, S. F. Kochegarov, and V. K. Subashiev, *Fiz. Tverd. Tela* **27**, 710 (1985) [*Sov. Phys. Solid State* **27**, 439 (1985)].
- ¹⁴P. M. Platzman and P. A. Wolff, *Waves and Interactions in Solid State Plasmas*, Academic Press, New York—London (1973).
- ¹⁵D. C. Hamilton and A. L. McWhorter, in *Light Scattering Spectra of Solids*, G. B. Wright (ed.), Springer-Verlag, New York (1969).
- ¹⁶J. M. Luttinger and W. Kohn, *Phys. Rev.* **97**, 869 (1955).
- ¹⁷S. D. Ganichev, E. L. Ivchenko, E. Yu. Perlin *et al.*, *Zh. Eksp. Teor. Fiz.* **91**, 1233 (1986) [*Sov. Phys. JETP* **64**, 729 (1986)].
- ¹⁸D. N. Zubarev, *Nonequilibrium Statistical Thermodynamics*, Consultants Bureau, New York (1974).
- ¹⁹A. I. Ansel'm, *Introduction to Semiconductor Theory*, Prentice-Hall, Englewood Cliffs, NJ (1981).
- ²⁰M. I. D'yakonov and V. I. Perel', *Zh. Eksp. Teor. Fiz.* **60**, 1954 (1971) [*Sov. Phys. JETP* **33**, 1053 (1971)].
- ²¹A. G. Aronov, G. E. Pikus, and A. N. Titkov, *Zh. Eksp. Teor. Fiz.* **84**, 1170 (1983) [*Sov. Phys. JETP* **57**, 680 (1983)].
- ²²N. H. March, *Collective Effect in Solids and Liquids*, IOP Pub., Philadelphia (1982).
- ²³A. M. Danishevskii, E. L. Ivchenko, S. F. Kochegarov, and M. I. Stepanova, *Pis'ma Zh. Eksp. Teor. Fiz.* **16**, 625 (1972) [*JETP Lett.* **16**, 440 (1972)].

Translated by David L. Book